NIST Practice Guide: Optical, Electron and Probe Microscopy Characterization of Carbon Nanotube Composites

Peter T Lillehei[1], Jae-Woo Kim[2], Cheol Park[3], Roy E Crooks[3] and Emilie J Siochi[1]

[1]Advanced Materials and Processing Branch, NASA Langley Research Center, Hampton, VA 23681 USA

[2] Science and Technology Corporation, Hampton, VA 23666 USA

[3] National Institute of Aerospace, Hampton, VA 23666 USA

Abstract

The development of tools to assess the dispersion of nanotubes in polymer matrices is based on the premise that one cannot improve what cannot be measured. An accurate assessment of the dispersion is the most critical factor in correlating the behavior of the final nanotube polymer composites to the nanostructure. This guide outlines the tools and the procedures used to assess the dispersion of nanotubes in a polymer matrix to allow for improvement and tailor-ability of the multifunctional properties of the composites.

1. Introduction The biggest challenge in translating multifunctional properties of nanotubes into improved composite structure performance is the difficulty in achieving an effective dispersion of the nanotubes in a polymer matrix [5-12]. A new set of characterization techniques is required to assess nanotube dispersion in polymer matrices.

The work presented herein lays a foundation for the systematic characterization of carbon nanotube composites via optical, electron, and probe microscopy.

Spectroscopic tools such as UV-VIS, IR, and Raman aid characterization by providing information on tube structure, functionalization, charge transfer between polymer and tubes, and even alignment of the tubes within the matrix [13-15]. However, these techniques are optically based and thus sample an ensemble of nanotubes because the minimum spot size is on the order of a few microns even in state-of-the-art instruments. While this information is useful and necessary to help understand the electrical, mechanical, and thermal data collected on the composites, additional information on how the nanotubes are actually being distributed within the polymer matrices is necessary to better understand the nanocomposite morphologies. This has led to the effort to develop these visual techniques to complement the optical spectroscopic techniques already commonly used to characterize nanotubes and nanocomposites.

The procedures used to assess dispersion of nanotubes in polymer matrices are outlined in Figure 1. The sample is first examined by optical microscopy to determine if any large-scale agglomerations are present. Figure 2 shows typical examples of optical micrographs of undesirable dispersion with SWNT aggregates and desirable uniform dispersion. If the sample passes optical microscopy standards, it is characterized as being optically dispersed (Figure 2(b)). It is then sufficient to state that the sample does not have any visual aggregation on the scale of approximately 1 μm or larger. To assess the aggregation, bundling, alignment, and local concentration gradients on a scale below 1

μm requires electron and probe microscopy techniques. These techniques include scanning electron microscopy (SEM), transmission electron microscopy (TEM), and scanning probe microscopy (SPM). Defining the quality of the dispersion on a scale below 1 μm is subjective. To suggest that a sample with 500 nm bundles is well dispersed would be misleading; therefore this guide outlines a procedure for the accurate assessment of bundle size, presence of agglomerations, and local concentration gradients on the scale below 1 μm.

The following sections describe the procedures and data that can be gleaned from the analytical techniques used, with a discussion pertaining to the limits of data interpretation. This will serve as a foundation for a robust and quantifiable nanotube composite characterization and will establish the limits for each analytical method.

2. Experimental Description

2.1 Instrumentation: Optical Microscopy

The optical microscope typically employs the use of light in the visible spectrum to generate a micrograph. Illumination of the samples above or below the sample determines the imaging mode, either reflection or transmission respectively. Ultraviolet illumination, polarizers, bright field/dark field imaging and optical filters enable enhanced imaging techniques.

Scanning Electron Microscopy

A scanning electron microscope employs the use of high-energy electrons, rather than photons, to image a surface. The sample must have a moderate electrical conductivity and

be stable in a high vacuum environment. Some new environmental scanning electron microscopes can handle low vacuum and high efficiency in-lens detectors can handle low conductivity samples, but for the most part conductivity and high vacuum stability are requirement. The primary electron beam is scanned over the surface generating secondary electrons (SE), backscattered electrons (BSE), and Auger electrons, in addition to x-rays. The Auger electrons and x-rays can be collected to give spectroscopic or chemical identification. The SE are collected to generate the topographical images. BSE are used generate maps based on atomic number. As the primary beam is scanned its position is mapped with respect to the number of SE, BSE, Auger electrons and x-rays recorded at their respective detectors.

Transmission Electron Microscopy

Transmission electron microscopes use a much more intense electron beam when compared to the beam used in SEM. These can be in the range of 200 – 300 keV for most commercial instruments. The collection of the SE, BSE, Auger electrons and x-rays can be achieved just as in SEM, but in addition the electron beam that passes entirely through the sample can be collected generating a transmission electron image. These electrons can be filtered based on how much energy was lost to the sample allowing for an additional spectroscopic technique. The scanning and transmission electron microscope's use of an electron beam to image a sample is a much higher resolution technique compared to optical microscopy, due to the much smaller characteristic wavelength of the electrons compared to the wavelength of visible photons. TEM, being the highest resolution technique, is typically capable of imaging samples up to atomic resolution.

Scanning Probe Microscopy

Scanning probe microscopes are a family of microscopes that have the following m,odes of operation: scanning tunneling microscopy (STM), atomic force microscopy (AFM), magnetic force microscopy (MFM), electric force microscopy (EFM), tunneling AFM (TUNA), current sensing AFM (CSAFM) magnetic resonance force microscopy (MRFM), electron spin resonance STM (ESR-STM), near field scanning optical microscopy (NSOM), and others. In all cases a small probe is scanned in close proximity to or in contact with a sample. Depending on the technique different aspects of the sample can be interrogated. STM uses an atomically sharp Pt or W probe in close proximity to a conductive sample under bais to record the tunneling current between the sample and the probe. AFM, MFM, EFM, TUNA and CSAFM use a MEMS based probe positioned in the near field to record the topography, magnetic field, electric field and tunneling current and current flow respectively. Spectroscopic data can be recorded in the adfvanced techniques such as MRFM and ESR-STM. NSOM also uses a MEMS based probe but can collect optical and spectroscopic data simultaneously.

2.2 Contrast generation: To assess the dispersion of nanotubes within a polymer matrix requires a method of generating contrast between the SWNT and the various polymer matrices. Regardless of the techniques used at least one single attribute of the nanotubes that differs from the host polymer is exploited in a manner to generate contrast between the nanotubes and the matrix. Whether it is optical transparency, electrical conductivity, or some other physical property of the nanotubes that differ from the polymer, contrast is generated between the polymer and the tubes by mapping the variations in the composite based on these properties.

Optical microscopy techniques are particularly valuable for assessing poor dispersion rapidly. Contrast is generated between the nanotubes and the polymer due to vastly different optical properties of the nanotubes and the host polymer. In either transmission or reflection the dispersion of the nanotubes on a large scale greater than 1 μm is easily assessed. Dispersion of the SWNT into aggregates or bundles smaller than the diffraction limit in the visible light range generally requires the use of electron and probe microscopy.

Contrast in SEM is due to the vastly different levels of conductivity of the SWNT and the polymer matrix. The composite builds up a charge from the primary electron beam and a stable electric field is generated on the surface of the sample. If the nanotubes are part of an electrical percolation network, they will dissipate the charge and lower the field to a less negative potential. If the electric field is stable, the percolation network can be imaged. Nanotubes disrupt the field in the surrounding polymer and appear as dark regions against the bright polymer matrix. Nanotubes at or near the surface, or penetrating into a cross-section, generate their own secondary electrons and appear as bright filaments in the image. This is shown in Figure 3 where SWNTs penetrate into a film and reverse contrast from bright to dark as they enter the polymer matrix; a few of these areas are highlighted by arrows in the Figure. If the local nanotube concentration is high enough, the electric field artifact will be overlaid on the secondary electron image. This explanation is consistent with the theory of electric field artifact imaging described by Goldstein et al. and others [16-19].

TEM studies were hindered by the weak contrast of the SWNTs within the composite, and two methods are used for contrast enhancement with some success. Image math and power spectrum filtering operations are used to enhance the periodicity contrast of the SWNT versus the polymer matrix. The adhesion and wetting of a polymer matrix on SWNT surfaces is assessed using energy filtered TEM (EFTEM) and electron energy loss spectroscopy (EELS) techniques [20].

In the SPM techniques contrast is generated by the paramagnetic and electrical behavior of the SWNTs [21]. Direct imaging of SWNT bundles and even individual tubes is achieved with the SPM technique of magnetic force microscopy (MFM). The MFM technique is an interleaved atomic force microscopy (AFM) procedure using a cantilever coated with a ferromagnetic material, typically cobalt. The AFM probe records the sample topography in a standard intermittent contact mode, then the probe is lifted a fixed distance above the recorded surface features and long range forces are measured as a phase shift on the freely oscillating cantilever. Tunneling AFM (TUNA) permits visualization of the percolation network by mapping local current flow from a sample and probe operating under a bias potential. This is similar to current sensing AFM (CAFM) but operates in the pA range.

3. Suggested Protocol

The investigation of 4 samples is described to illustrate the characterization procedure (see table 1). It is important to note that the samples are all SWNT-polyimide composites

made under various processing conditions or with varying concentrations of nanotubes. Details of sample preparation are documented elsewhere [5, 6, 8, 20].

Characterization of SWNT dispersion is performed in a top down approach. Optical microscopy is used as a screening tool for electron and probe microscopy. Table 1 shows an example of the optical microscopy images taken in transmission for each sample.

The samples are each prepared for optical microscopy by either casting a film or preparing a thin section. If the sample is transparent, transmission illumination is a very good and quick method to capture the large-scale bulk dispersion.). For a uniformly dispersed composite, at least 200x magnification is recommended. Agglomerations on a scale large than 1 μm are easily visible with this technique. If the sample is not transparent, illumination via reflection does give some indication of the large-scale dispersion but the sample will need to be examined on the surface and in cross-section to assess the dispersion throughout the bulk of the sample.

Sample 1 was processed in a direct mixing procedure and large-scale agglomerates could be clearly seen. The percent optical transmission of this sample is very low, on the order of 1% at 500 nm. Sample 2 was made with the same formulation but the nanotubes were incorporated into the composite via an *in-situ* polymerization technique [5, 8]. In contrast to the direct mixing technique, this sample has a 32% transmission at 500 nm with the same thickness. Sample 2 is considered "optically dispersed." If the composite does not need further optimization for the intended application, optical characterization is usually

sufficient. However, if optimization of mechanical, electrical, or thermal properties is required, a more in-depth analysis of the dispersion is needed.

Samples 2, 3, and 4 illustrate the need for characterization beyond the optical microscope. These samples are all considered optically dispersed though they have different mechanical and electrical properties. It is rationalized that the resulting differences in mechanical and electrical properties are due to varying levels of dispersion of the SWNTs within the composite. Differences in samples 2, 3 and 4 are visible with optical microscopy but it is not clear what is the cause of the differences. Scratches, dust, entrapped air bubbles and catalyst particles along with nanotube agglomerates are visible in all the images. These defects are clearly visible with this technique and need to be recorded to give an overview of the nanotube distribution and the overall defect density. What is not clear is how the majority of the tubes are distributing themselves between these defects.

To investigate the difference between samples 2, 3 and 4 beyond the optically dispersed limit requires an investigation of the nature of the dispersion below the 1-μm scale. The main tool employed in this investigation is the high resolution FE-SEM (HR-FESEM). This tool creates a stable electric field in most polymers and generates a very high collection efficiency of the secondary electrons, such that samples just exceeding the electrical percolation threshold are easily imaged without the typical thin metal coating. Figure 4 shows samples 1-4 normal to the film surface and in cross-section. Aggregates and an inhomogeneous distribution are visible in the film and cross-section of samples 1-

3, whereas a uniform distribution with no visible aggregation is seen in sample 4. At this point it is important to note that the only difference between samples 3 (Figures 4e and 4f) and 4 (Figures 4g and 4h) is the SWNT manufacturing process. Sample 3 was made by the HiPco process and sample 4 was made by a laser ablation technique. The HR-FESEM is powerful enough to detect the dispersion differences due only to the SWNT manufacturing process.

The electron microscopy investigations of these composites requires very little preparation. Samples are mounted on the specimen stage using a conductive adhesive, typically a silver paste. It is important that the imaging surface has at least a moderate conductivity ($>10^{-8}$ S/cm). The samples are not coated with a conductive layer, but rather inserted directly into the specimen chamber without any additional preparation. The accelerating voltage of the primary electron beam is set to as low of a voltage as is practical for imaging the specimen. Typically this process begins somewhere around 0.5 keV and is brought up until a contrast is generated between the conductive nanotubes and the non-conducting host matrix. If contrast cannot be established, a variation in the scan rate may be necessary to establish the contrast.

The ability to image a network of nanotubes is not limited to HR-FESEM. Conventional W-filament SEMs are more than capable of imaging such networks as shown in Figure 5. Typically, great efforts are employed to reduce the presence of such image artifacts, as those arising from a charge build-up that generates a large electric field. However, for these studies the electric field artifact is the tool exploited to image nanotubes that are

part of the percolation network. Thus uncoated SWNT-polymer composite samples are directly inserted into the electron microscope and grounded to a sample stage with silver paste. With SEM, details on SWNT aggregation and distribution are easily determined and estimates of the bundle sizes can be made as well.

More quantitative information on the size of individual tubes and how they bundle requires the use of the TEM. SWNT-polymer composite samples typically require microtoming or ion milling to create thin sections suitable for TEM imaging. Figure 6 shows a SWNT-polymer composite where the individual tubes in bundles are clearly visible in the polymer under high magnification. It was observed that the tubes were not locked into a single rope-like configuration, but pass from one bundle to the next.

Novel scanning probe techniques are shown in Figure 7. MFM characterized the dispersion of the SWNT in polymer composites by mapping the magnetic field at a fixed height above the sample [21]. The TUNA technique was complementary to MFM, though much more straightforward. These SPM techniques are of particular interest because they are simple approaches that do not require an electron microscope. The distribution of SWNTs in the polymer matrix are clearly visible in both the MFM (Figure 7(b, d)) and TUNA images (Figure 7(c, e)) [26].

The MFM requires the use of a Co/Cr coated AFM cantilever. Contrast is enhanced with the thicker Co coatings found on high moment MFM cantilevers (~100 nm Co). These thick coatings increase the radius of the MFM tip and degrade the spatial resolution.

Careful consideration of spatial resolution versus contrast generation needs to be balanced for the MFM imaging. Once a suitable cantilever that gives adequate contrast and spatial resolution is found, the MFM probe is magnetized by placing the probe over a strong magnet for several minutes. The sample is then placed on the scanner above a strong magnet. The paramagnetic nanotubes, which are a subset of the total nanotube population, disrupt the local magnetic field from the strong magnet under the sample. These nanotubes are imaged with the MFM in an interleave mode. The sample topography is first scanned and then the probe is raised a fixed distance, typically 7 – 15 nm, above the surface and the magnetic field gradient is then recorded. These small lift heights require that the sample be relatively flat before imaging. Thin films formed by spin casting or knife coating work best.

The TUNA procedure requires the use of a conductive AFM probe. The restrictions on the coatings are limited so long as the probe is conductive. As such the conductive probes can have a much sharper tip radius when compared to the MFM probes. The TUNA procedure is also a direct technique, not requiring an interleave or lift mode. The sample topography and tunneling current are recorded simultaneously at each pixel. Additionally, the bias voltage can be scanned to enhance or reduce contrast in the current image. This scanning of the bias voltage can even bring different portions of the network into view, allowing for a more detailed analysis of the network as a function of applied voltage.

4. Conclusions

The use of conventional microscopy techniques enables the investigation of carbon nanotube dispersions in polymer composites. Subtle differences at the nanoscale produce large changes in the composite and necessitate the closer examination of these materials by electron and probe microscopy. The end result is a method of SWNT composite investigation that involves examination by optical microscopy to first determine if SWNT dispersion is poor. Second, the SEM is used on the composite surface and cross-section to determine bulk dispersion. If additional information is required beyond the degree of dispersion, then direct imaging of the nanotubes by TEM yields information on the size and packing of individual bundles. The use of FE-SEM over conventional SEM is not necessary to assess the dispersion, but it can be beneficial for composites with limited conductivity or samples susceptible to significant beam damage. Probe microscopy techniques are useful tools to investigate nanotube dispersion and provide complementary information to electron microscopy.

5. Acknowledgement

6. References

[1] National Aeronautics and Space Administration Aeronautics Blueprint http://www.aeronautics.nasa.gov/aboutus/tf/aero_blueprint/index.html 2003

[2] Cheng H M, Li F, Sun X, Brown S D M, Pimenta M A, Marucci A, Dresselhaus G and Dresselhaus M S 1998 *Chem. Phys. Lett.* **289** 602

[3] Ajayan P M 1999 *Chem. Rev.* **99** 1787

[4]   Zhu H W, Xu C L, Wu D H, Wei B Q, Vajtal R and Ajayan P M 2002 *Science* **296** 884

[5]   Park C, Ounaies Z, Watson K A, Crooks R E, Smith J G Jr., Lowther S E, Connell J W, Siochi E J, Harrison J S and St. Clair T L 2002 *Chem. Phys. Lett.* **364** 303

[6]   Park C, Ounaies Z, Watson K A, Pawlowski K J, Lowther S E, Connell J W, Siochi E J, Harrison J S and St. Clair T L 2002 *NASA/CR* 2002-211940

[7]   Kumar S, Dang T D, Arnold F E, Bhattacharyya A R, Min B G, Zhang X, Vaia R A, Park C, Adams W W, Hauge R H, Smalley R E, Ramesh S and Willis P A 2002 *Macromolecules* **35** 9039

[8]   Ounaies Z, Park C, Wise K E, Siochi E J and Harrison J S 2003 *Composites Sci. and Technol.* **63** 1637

[9]   Siochi E J, Lillehei P T, Wise K E, Park C and Rouse J H 2003 *SEM Annual Conference MEMS/NEMS*

[10]   Siochi E J, Working D C, Park C, Lillehei P T, Rouse J H, Topping C C, Bhattacharyya A and Kumar S 2004 *Composites Part B* **35** (5) 439

[11]   Smith J G Jr., Connell J W, Delozier D M, Lillehei P T, Watson K A, Lin Y, Zhou B and Sun Y-P 2004 *Polymer* **45** 825

[12]   Delozier D M, Tigelaar D M, Watson K A, Smith J G Jr., Lillehei P T and Connell J W 2004 *SAMPE Symposium & Exhibition*

[13]   Haggenmueller R, Gommans H H, Rinzler A G, Fischer J E and Winey K I 2000 *Chem. Phys. Lett.* **330** 219

14

[14] Thostensona E T, Renb Z and Choua T-W 2001 *Composites Sci. and Technol.* **61** 1899

[15] Strano M S, Dyke C A, Usrey M L, Barone P W, Allen M J, Shan H, Kittrell C, Hauge R H, Tour J M and Smalley R E 2003 *Science* **301** 1519

[16] Knoll M 1941 *Naturwissenschaften* **29** 335

[17] Kong J, Soh H T, Cassell A M, Quate C F and Dai H 1998 *Nature* **395** 878

[18] Zhang Y, Chang A, Cao J, Wang Q, Kim W, Li Y, Morris N, Yenilmez E, Kong J and Dai H 2001 *Appl. Phys. Lett.* **79** 3155

[19] Goldstein J I, Lyman C E, Newbury D E, Lifshin E, Echlin P, Sawyer L, Joy D C and Michael J R 2003 *Scanning Electron Microscopy and X-Ray Microanalysis* **3**[rd] **ed**. Kluwer Academic/Plenum Publishers, New York Chapter 5.

[20] Park C, Crooks R E, Siochi E J, Harrison J S, Evans N, Kenik E 2003 *Nanotechnology* **14** L11–L14

[21] Lillehei P T, Park C, Rouse J H and Siochi E J 2002 *Nano. Lett.* **2** 827

[22] Viswanathan R and Heaney M B 1995 *Phys. Rev. Lett.* **75** 4433

[23] Simpson J, Ounaies Z and Fay C 1997 *Mat. Res. Soc. Symp. Proc.* **459** 53

[24] Wise K E, Park C, Siochi E J, Harrison J S 2004 *Chem. Phys. Lett.* **391** 207

[25] St. Clair A K and St. Clair T L 1986 *U.S. Patent* 4,603,061

[26] The topographical image and the MFM image were obtained simultaneously, while the TUNA image was taken on the same sample after the tip was exchanged. Thus the MFM and TUNA images are at slightly different locations on the sample.

Figures

Figure 1. Guide to assess the dispersion of SWNT in polymer matrices.

Figure 2. Optical micrographs: (a) Undesirable dispersion with SWNT aggregates, (b) desirable uniform SWNT dispersion (optically dispersed) in a polyimide matrix.

Figure 3. HR-FESEM images of a SWNT-CP2 composite in cross-section showing the SWNTs penetrating out of the film. Nanotubes that are penetrating out of the cross-section generate their own secondary electrons and appear as bright filaments in the image. The arrows highlight points where the nanotubes penetrate into the polymer and disrupt the electric field in the surrounding polymer. The contrast is then reversed and the nanotubes appear as dark regions against the bright polymer matrix.

Table 1. Optical microscopy images of samples 1-4.

Figure 4. HR-FESEM images on the dispersion quality of samples 1-4. (a) Surface and (b) cross-section of sample 1 showing poor dispersion quality. Optical microscopy already showed this sample had a poor dispersion; shown here for comparison. (c) Surface and (d) cross-section of sample 2 showing improved dispersion over the direct mixing technique. (e) Surface and (f) cross-section of sample 3 showing an improved dispersion from using the β-CN polymer. Dispersion is still not ideal due to poor quality of SWNT. (g) Surface and (h) cross-section of sample 4 showing nearly 100% dispersion, no visible aggregates, very small bundles, and no resin rich areas.

Figure 5. SEM image of a SWNT-CP2 composite showing the same electric field artifact contrast as seen with the HR-FESEM.

Figure 6. TEM of SWNT-CP2 directly showing individual tubes in the polymer matrix.

Figure 7. Scanning probe microscopy images complementary to electron microscopy of 2 SWNT-β-CN composites (a-c: 0.5% SWNT β-CN, d-f: 2% SWNT β-CN). (a,d)Topography, (b,e) MFM images and (c,f) TUNA images.
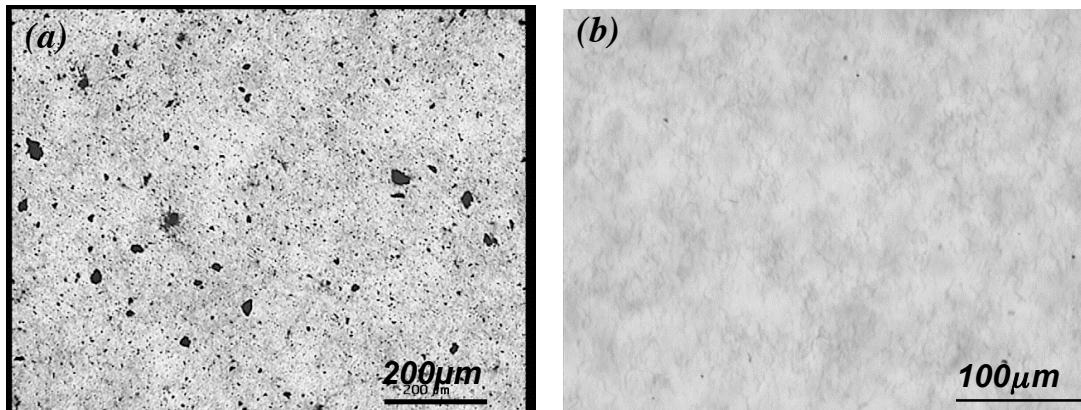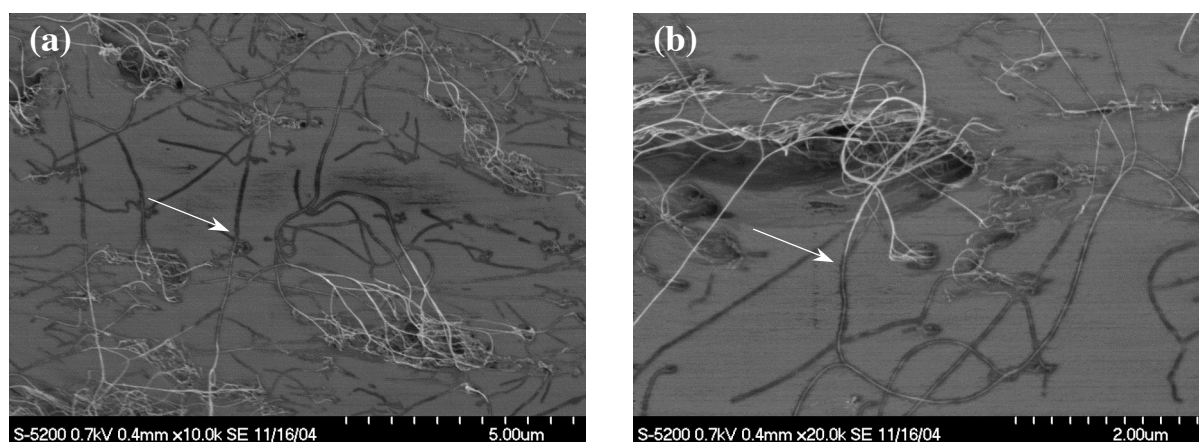
Figure 1
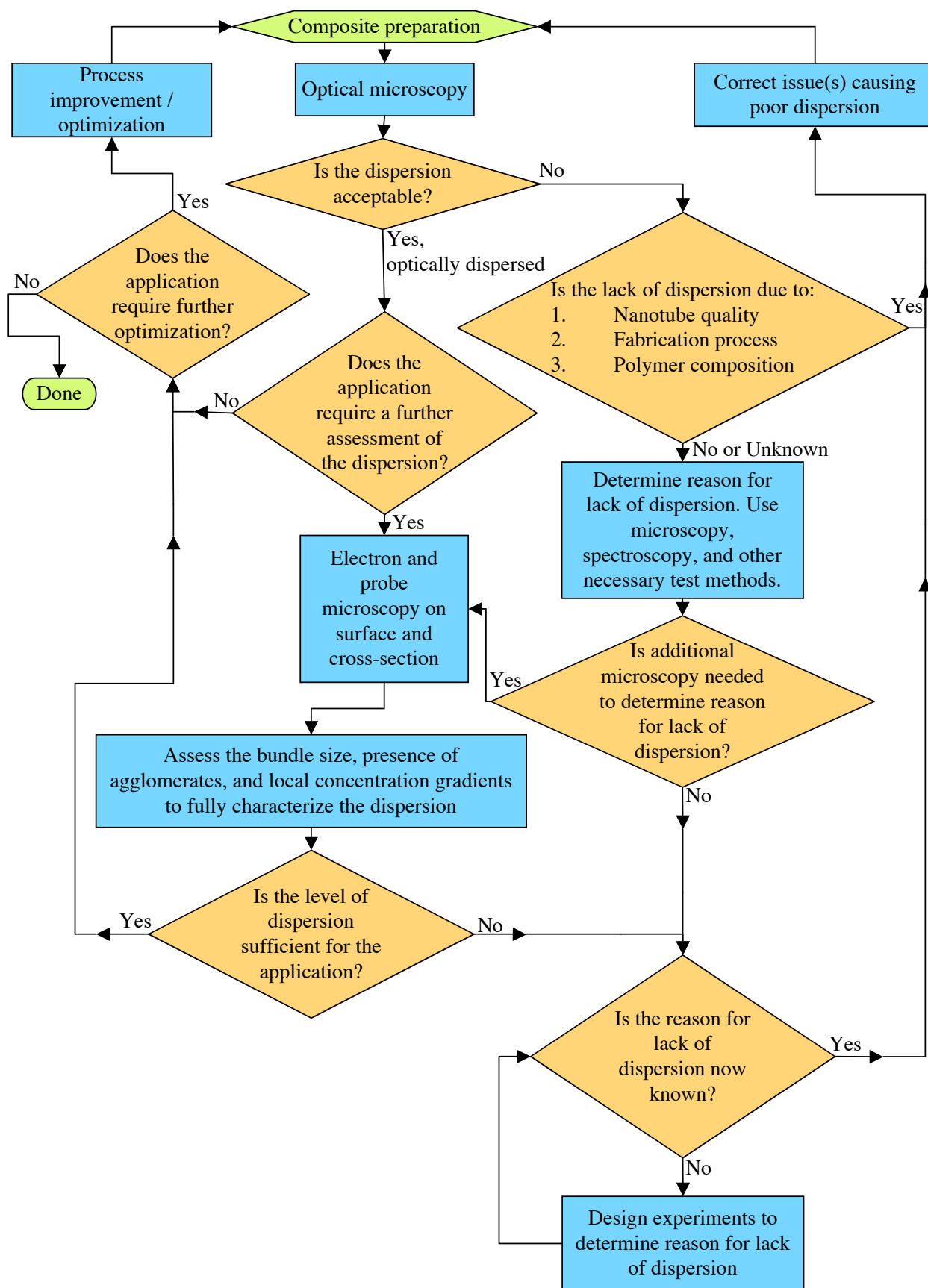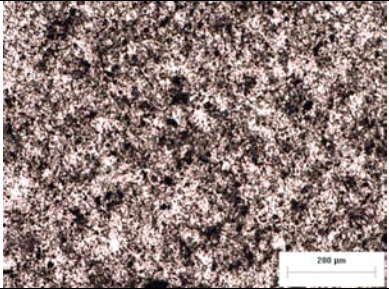
Figure 2.

Figure 3.

Table 1.
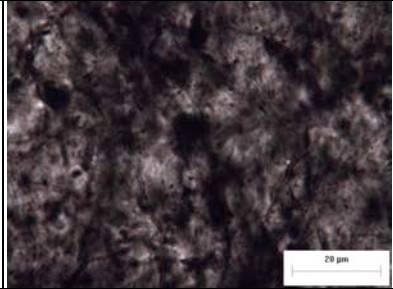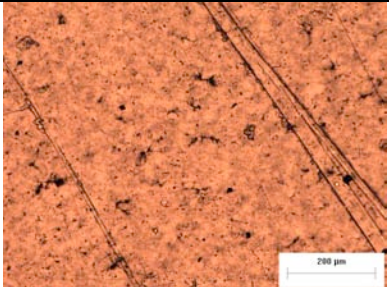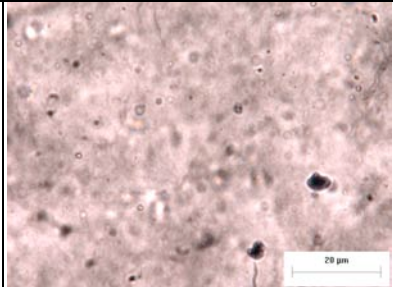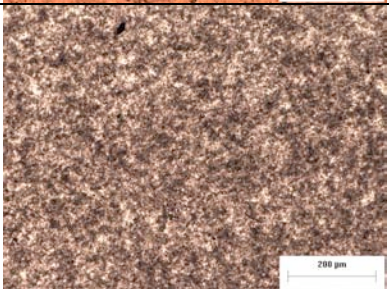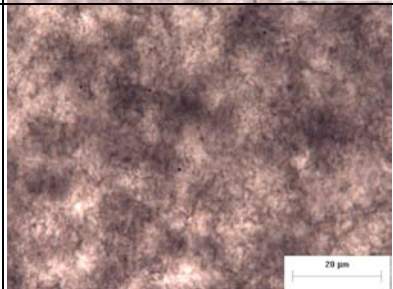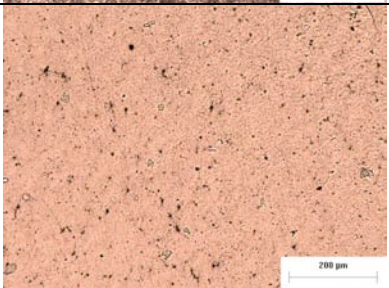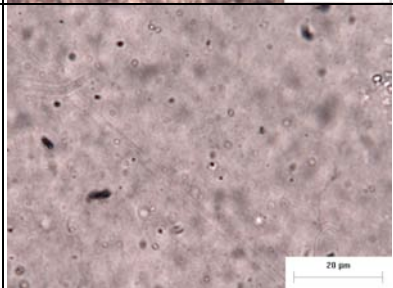
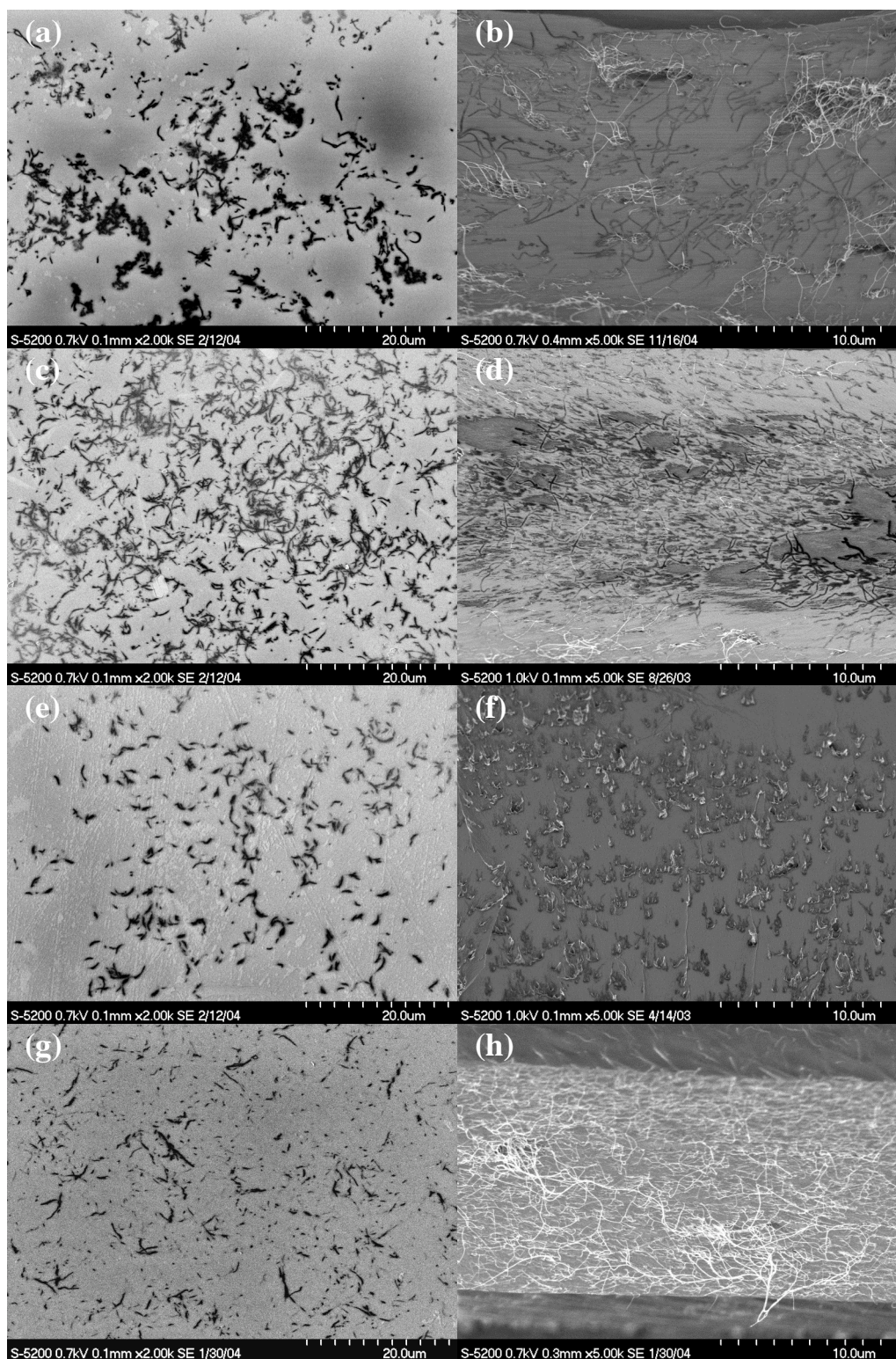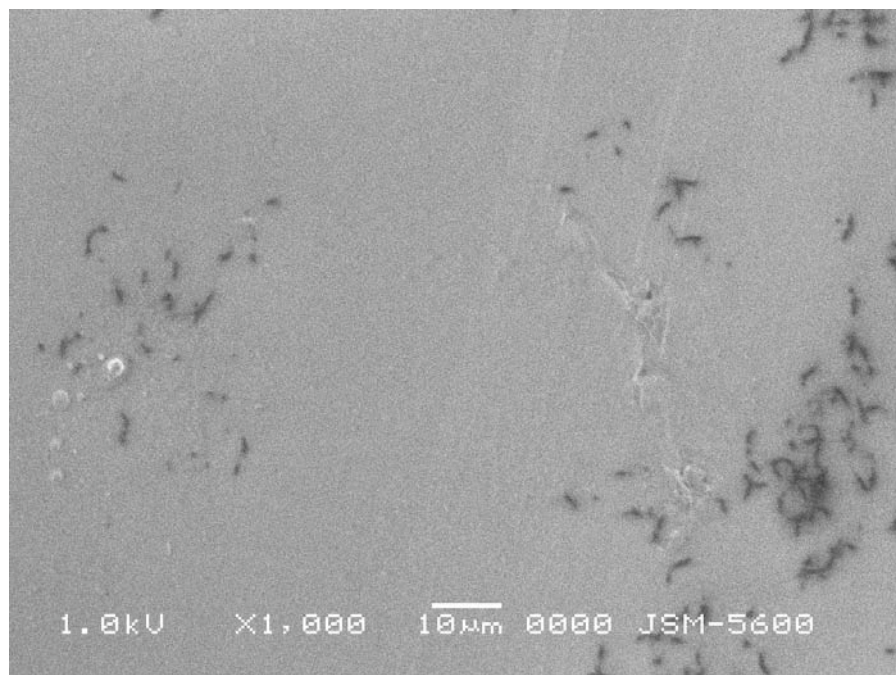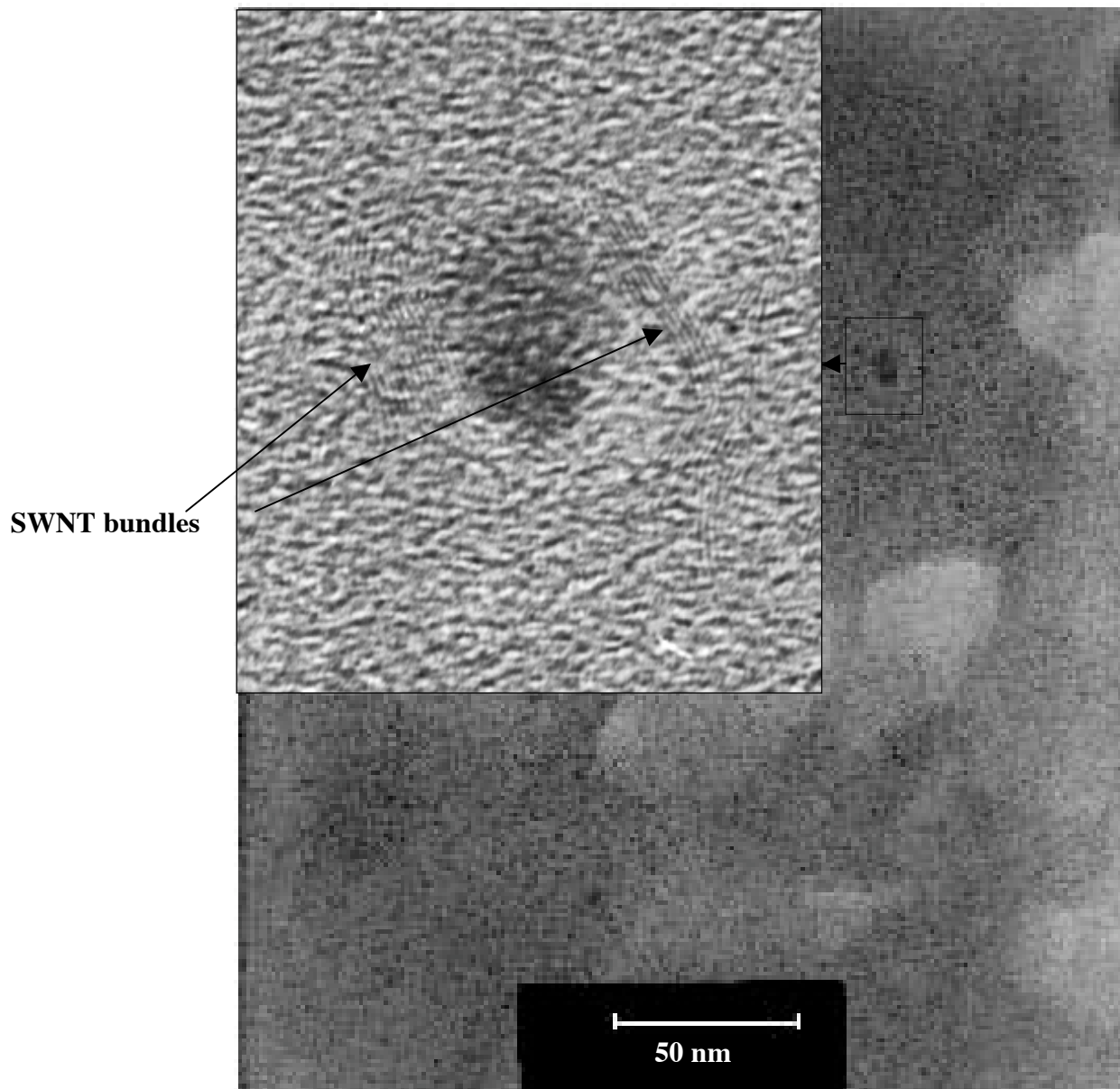| Sample	Mixing Conditions	Optical Microscopy	
Sample 1 1% SWNT CP2	Direct Mix		
Sample 2 1% SWNT CP2	*In-situ* polymerization under sonication		
Sample 3 0.5% SWNT β-CN	*In-situ* polymerization with HiPco SWNT		
Sample 4 0.5% SWNT β-CN	*In-situ* polymerization with laser ablation SWNT		

Figure 4.

Lillehei *et al*.

Figure 5.

Figure 6.

Lillehei *et al.*

Figure 7.